Supplementary

Appendix 1 The specific study setting of the research

The First Teaching Hospital of Tianjin University of Traditional Chinese Medicine is a Class III Grade A general hospital. The comprehensive implementation of this study mainly depends on the hospital's specialized resources, equipment conditions, and standardized diagnosis and treatment systems.

The specific details are as follows:

Core Departments Supporting the Research

This study is supported by two core departments of the hospital, namely the Pediatric Respiratory Department and the Radiology Department. The Pediatric Respiratory Department has developed standardized diagnostic and treatment systems for pediatric respiratory infectious diseases, such as *Mycoplasma pneumoniae* pneumonia (MPP), and provided a cohort of pediatric patients that meets the inclusion criteria for this study. The Radiology Department is staffed with professional technical personnel and has established standardized operating procedures for low-dose chest CT scans in children, thereby ensuring the uniformity and standardization of scanning operations.

Equipment configuration

The radiology department is furnished with a state-of-the-art 256-slice volumetric CT scanner (Revolution Apex CT, GE Healthcare). This scanner offers the hardware basis for the acquisition of low-dose chest CT data in the study, along with the subsequent multi-algorithm image reconstruction utilizing adaptive statistical iterative reconstruction (ASIR) and deep learning image reconstruction (DLIR). This device is completely compatible with the GE original reconstruction algorithms (ASIR, DLIR - TrueFidelity) adopted in the study.

Data management and retrieval capabilities

The hospital is equipped with a comprehensive Electronic Medical Record System (EMRs) and a Picture Archiving and Communication System (PACS). Researchers are capable of retrieving data from pediatric patients who were clinically diagnosed with pneumonia and underwent chest CT examinations during the study period (September 2023—March 2024) through these two systems. The data encompasses basic information, laboratory test outcomes, and imaging materials, providing crucial support for patient screening and data collection in retrospective studies.

Ethical approval and research standards

This study was formally approved by the Ethics Committee of the First Teaching Hospital of Tianjin University of Traditional Chinese Medicine (Approval No.: TYLL2024[Z] 025). As the study was designed as a retrospective study, the Ethics Committee exempted the requirement for written informed consent from patients. The entire study process adhered to the ethical standards of clinical research.

Patient screening workflow in clinical practice

The diagnostic and treatment workflow within this research scenario offers a practical framework for patient screening. In the case of children suspected of having MPP, hospitals generally commence with X-ray screening. Subsequently, clinical manifestations and pulmonary auscultation results are taken into account. Prior to conducting a chest CT examination, consent from the family is obtained. Some families may directly opt for CT scans to prevent secondary radiation exposure. This actual clinical practice is also integrated into the description of the patient enrollment background in the study.

https://dx.doi.org/10.21037/tp-2025-1-923

Appendix 2 The flowchart for participant recruitment

The flowchart for participant recruitment encompassed three fundamental steps:

Preliminary screening

EMRs and PACS of the hospital were employed to retrieve all pediatric patients clinically diagnosed with pneumonia who underwent chest CT during the study period. Subsequently, the patients' basic information (including age, gender, body mass index [BMI], admission time, etc.) and examination data were initially gathered.

Inclusion and exclusion verification

Two independent researchers with professional expertise in pediatric radiology verified the inclusion and exclusion criteria of the screened patients through a comprehensive review of complete medical records, laboratory test reports, and imaging data. Discrepancies were resolved through consultation with a senior chief radiologist possessing over 20 years of clinical experience in pediatric respiratory diseases.

Final enrollment

Patients who fulfilled all inclusion criteria and did not meet any exclusion criteria were incorporated into the final study cohort. A standardized case report form was employed to gather and document all relevant data of the enrolled patients, thereby ensuring data comprehensiveness and precision.

Appendix 3 Detailed descriptions of the inclusion and exclusion criteria

Inclusion criteria: (a) pediatric patients under 18 years old with pneumonia admitted to our hospital for the first time; (b) who underwent chest CT scan at our hospital for the first time during the admission period; (c) serum MP-IgM antibody test result was positive; all results of the seven-item respiratory pathogen antibody test (Cpn-IgM, RSV-IgM, Adv-IgM, FluA-IgM, FluB-IgM, and PIV-IgM) were negative; (d) complete raw CT data that can support multi-algorithm reconstruction were available..

Exclusion criteria: (a) pediatric patients with incomplete clinical information (eg. fever, cough, wheezing, etc.), laboratory test data (MPP-specific laboratory markers and inflammation-related laboratory markers) or imaging data, including children who refused serum MP-IgM assay or seven-item respiratory antibody test; (b) who were unable to cooperate to complete the chest CT scan (e.g., severe restlessness without sedation, inability to complete breath-hold training), resulting in unqualified image quality that cannot be used for subsequent analysis; (c) considering the close correlation between radiation dose and weight, the pediatric patients with BMI ≥25 kg/m^2 to the World Health Organization (WHO) BMI classification for children and adolescents were excluded; (d) patients with unsuccessful CT image reconstruction using the preset algorithms (ASIR 0%/50%/80%, DLIR-Low/Medium/High) due to equipment or data reasons; (e) patients with a history of other severe pulmonary diseases (e.g., bronchopulmonary dysplasia, interstitial lung disease) or systemic diseases (e.g., immunodeficiency, congenital heart disease) that may affect lung imaging manifestations.

Appendix 4 Detailed steps for sample size calculation of this study

Overview

The sample size calculation was performed using IBM SPSS Statistics 26.0 software, with the contrast-to-noise ratio (CNR) of MPP lesions as the core outcome measure. This choice was based on the primary study objective: comparing image quality across different reconstruction algorithms, where CNR directly reflects the ability to distinguish MPP lesions from normal lung parenchyma— a critical metric for clinical diagnosis.

Key preset parameters were defined a priori to ensure statistical rigor:

- Significance level (α): 0.05 (two-tailed test)
- Statistical power (1–β): 0.8 (to minimize type II errors)

https://dx.doi.org/10.21037/tp-2025-1-923

- Core comparison: DLIR at high-strength level (DLIR-H) *vs.* ASIR at 80% blending factor (ASIR-80%), as these represent the highest-performance variants of each algorithm family.

Effect size determination and validation

Effect size quantifies the magnitude of the expected difference between groups, a prerequisite for reliable sample size estimation.

Initial effect size calculation

To avoid bias from small pre-experimental samples, the effect size was initially derived from the complete dataset of 142 enrolled patients (post-hoc calculation). For this:

- Descriptive statistics (mean, standard deviation [SD], combined SD) of MPP lesion CNR were extracted for all six reconstruction algorithms (ASIR-0%, ASIR-50%, ASIR-80%, DLIR-L, DLIR-M, DLIR-H).
- For multi-group comparisons (all six algorithms), the effect size "f" was calculated via one-way analysis of variance (ANOVA), yielding f=0.43.
- For the core two-group comparison (DLIR-H *vs.* ASIR-80%), Cohen's d (effect size for independent samples) was computed, resulting in d=0.33.

Cross-validation with prior literature

To enhance the credibility of the post-hoc effect size, we validated it against a relevant prior study (Zhang K, Shi X, Xie SS, Sun JH, Liu ZH, Zhang S, Song JY, Shen W. Deep learning image reconstruction in pediatric abdominal and chest computed tomography: a comparison of image quality and radiation dose. Quantitative Imaging in Medicine and Surgery. 2022 Jun;12(6):3238-3250. doi: 10.21037/qims-21-936), which compared DLIR and ASIR algorithms in pediatric chest CT. This study reported an effect size of f=0.41 for CNR-based comparisons, consistent with our calculated f=0.43. This cross-validation confirmed that our effect size was neither overestimated nor underestimated, supporting the rationality of subsequent sample size calculations.

Multi-dimensional sample size calculation

Sample size was estimated across four complementary dimensions to ensure adequacy for all primary and secondary study outcomes:

Dimension 1: Multi-group reconstruction algorithm comparison

A one-way ANOVA power analysis was conducted to estimate the minimum sample size required to detect differences in CNR across the six algorithm groups. Input parameters included:

- Number of groups: 6
- Effect size (f): 0.43
- α=0.05, power=0.8

Result: The minimum sample size required per group was 10, corresponding to a total minimum sample size of 60 (10 patients × 6 groups).

Dimension 2: Core two-group comparison (DLIR-H *vs.* ASIR-80%)

A two-sample *t*-test power analysis was performed to focus on the primary research question. Input parameters included:

- Sample size ratio (DLIR-H *vs.* ASIR-80%): 1:1 (self-control design, as all patients underwent both reconstructions)
- Cohen's d: 0.33
- α=0.05, power=0.8

Result: The minimum sample size required per group was 58, corresponding to a total minimum sample size of 58 (since each patient contributed data to both groups in the self-control design).

Dimension 3: Qualitative subjective score comparison

Subjective image quality scores (5-point scale) were dichotomized into "high quality" (4-5 points) and "low quality" (1-3 points) to facilitate a two-sample proportion chi-square test power analysis. Input parameters included:

https://dx.doi.org/10.21037/tp-2025-1-923

- Expected proportion of high-quality scores in DLIR-H group: 85% (based on pilot observations)
- Expected proportion of high-quality scores in ASIR-80% group: 65%
- α=0.05, power=0.8

Result: The minimum sample size required was 52 patients to detect a statistically significant difference in the proportion of high-quality scores between groups.

Dimension 4: Observer consistency test

Intraclass correlation coefficient (ICC) reliability analysis was used to estimate the minimum sample size required to validate inter- and intra-observer consistency for subjective scoring. Based on methodological guidelines for ICC analysis (ICC > 0.7 defined as substantial agreement), the minimum sample size required to achieve reliable consistency estimates was 50 patients.

Sample size rationality validation

Adequacy of enrolled sample size

The final enrolled sample size (142 patients) exceeded the minimum requirements derived from all four dimensions:

- 142 > 60 (multi-group comparison)
- 142 > 58 (core two-group comparison)
- 142 > 52 (subjective score comparison)
- 142 > 50 (observer consistency test)

A post-hoc power analysis confirmed that the enrolled sample size provided a statistical power of 0.98 (far exceeding the preset 0.8), ensuring robust detection of even small-to-moderate effect sizes.

Consideration of potential biases

To account for common biases in clinical observational studies (e.g., missing data, non-compliant image quality, protocol deviations), we incorporated a 10% "buffer" into the sample size estimation. The enrolled 142 patients fully accommodated this buffer, ensuring that even if up to 14 patients were excluded post-hoc, the remaining sample size (128) would still maintain adequate statistical power ($\geq$ 0.85).

Sensitivity analysis

A sensitivity analysis was conducted to verify the stability of the sample size estimate across different outcome measures. This involved:

- Performing principal component analysis (PCA) on three quantitative image quality indicators: MPP lesion CNR, lung parenchyma signal-to-noise ratio (SNR), and background noise (SD value).
- PCA reduced the three correlated indicators into a single composite score (weighted by the variance contribution rate of each principal component), which was used as an auxiliary outcome measure.
- Repeating the sample size calculation using this composite score yielded a minimum required sample size of 55, which was consistent with the prior estimates.

This sensitivity analysis confirmed that our sample size was robust and not dependent on a single outcome measure, further supporting its adequacy.

Conclusion

Based on multi-dimensional calculations, cross-validation with prior literature, and sensitivity analysis, the minimum sample size required for the study was determined to be 60 patients. The final enrollment of 142 patients provided sufficient statistical power (0.98) to address all study objectives, including multi-group algorithm comparisons, core two-group contrasts, subjective score analysis, and observer consistency validation. This sample size balanced statistical rigor with practical feasibility, ensuring reliable and generalizable results.

https://dx.doi.org/10.21037/tp-2025-1-923

Appendix 5 Specific CT scan procedures in the current study

The pediatric patients held their breath during the examination. All patients were scanned craniocaudally in the supine position with the bilateral upper limbs raised over the head. And the longitudinal alignment of the positioning cursor was aligned on the central sagittal plane of the sternoclaviculare. The orthotopic scanning was performed firstly, and then the scanning baseline and range were confirmed according to the scout view. The chest was scanned from the tip of the lung to the angle of the pulmonary septum. The scanning parameters of low-dose CT were as follows: axial scan, collimation 80-140 mm, rotation time 280-500 ms, display field of view 200-350 mm, image matrix 512×512, and 5 mm slice thickness/interval. The tube voltage and tube current were set according to different weights, which were 70 kV, 135 mA (6.0-7.5 kg); 70 kV, 155 mA (7.5-9.5 kg); 100 kV, 150 mA (9.5-11.5 kg); 100 kV, 170 mA (11.5-14.5 kg); 100 kV, 190 mA (14.5-18.5 kg); 100 kV, 170 mA (18.5-22.5 kg); 100 kV, 190 mA (22.5-31.5 kg); 100 kV, 220 mA (31.5-40.5 kg); and 120 kV, 175 mA (40.5-55.0 kg), respectively.

Appendix 6 Regulations for the low-dose CT scanning protocol in this study

The GE Healthcare 256-slice volume CT scanner (Revolution Apex CT) was used in the current study. The manufacturer of this device has set a low-dose CT scanning protocol initially and provided the corresponding instruction manual. That is to say, our hospital has always used low-dose scanning protocol for pediatric chest CT scan. Therefore, even in this retrospective study, the data included in this experiment met the preset requirements. On the other hand, an article titled "Deep Learning Image Reconstruction for CT: Technical Principles and Clinical Prospects" published in Radiology in 2023 also introduced the low-dose scanning of the Revolution Apex CT device, which indirectly proved the low-dose feature of this machine's scanning.

On the other hand, referring to three relevant guidelines, namely "Chinese Expert Consensus on Radiation Dose Standards for Pediatric CT Examinations" published in Chinese Journal of Radiology in 2024, "Preliminary Investigation on the Current Situation of Radiation Dose in Pediatric CT Scans and Diagnostic Reference Levels" published in 2022, and "Expert Consensus on Standardization of Chest CT Scanning" published by the Radiological Technology Branch of the Chinese Medical Association in 2020 we found that the radiation dose generated during the pediatric chest CT scans in this study was lower than the relevant reference levels in the guidelines.

In summary, we believe that the radiation dose adopted from the beginning of this study met the low-dose requirement. It should be emphasized here that this study was not a multi-group controlled experiment. That is, due to the limitations of the retrospective nature and ethical requirements, this study did not design a comparison of different CT images under multiple groups of different radiation doses. We were more concerned about comparing the image quality after different reconstruction algorithms using the GE Healthcare 256-slice low-dose Revolution Apex CT scanner, hoping to enhance the confidence of radiologists in diagnosing pediatric chest CT images. On the other hand, the GE Healthcare 256-slice Revolution Apex CT scanner is still a new device in China and has not been widely promoted in major hospitals. Our hospital and GE company also look forward to more, better, and more accurate experiments to gain public recognition for this device.

Appendix 7 Specific measurement and calculation methods of size specific dose estimate (SSDE)

Firstly, according to American Association of Physicists in Medicine (AAPM) Report 204, we selected the middle layer in the chest CT scan first to measure the anterior-posterior (AP) line and lateral (LAT) line of the thoracic cage. An intermediate layer containing all lung tissue from the tip of the lung to the diaphragmatic angle was selected; where, AP value is the distance from the anterior chest wall to the posterior margin of the corresponding vertebral body (avoiding the subcutaneous fat layer), and LAT value is the maximum distance between the two pleural cavities. The lines were measured using RadiAnt Digital Imaging and Communications in Medicine (DICOM) Viewer software. All lines were measured three times by two graduate students, and the average was taken as the final result. Both inter-observer and intra-observer consistency analysis were carried out to ensure the accuracy of the results. The effective diameter (ED) was calculated through the formula "ED=$\sqrt{AP \times ALT}$". By consulting the table in AAPM Report 204, the conversion coefficient f_{size} was obtained. When ED is between table values, linear interpolation method is used to obtain it. Finally, the SSDE is calculated by formula "SSDE = $f_{size} \times CTDI_{vol}$". $CTDI_{vol}$ is the volume CT dose index.

The linear interpolation method is supplemented here. According to AAPM Report 204, when the effective diameter (unit: cm) increased from 10 to 32, the *f* size showed a continuous decreasing trend: 1.50 at 10 cm, 1.30 at 12 cm, 1.15 at 14 cm, and 1.00 at 16 cm; subsequently,

https://dx.doi.org/10.21037/tp-2025-1-923

0.90 at 18 cm, 0.85 at 20 cm, 0.75 at 22 cm, 0.70 at 24 cm, 0.65 at 26 cm, 0.60 at 28 cm, 0.55 at 30 cm, and 0.50 at 32 cm. Assume that the effective diameter of the patient is 19 cm; Looking up the table, we find that 19 cm is between 18 cm and 20 cm, and the corresponding f_{size} values are 0.90 and 0.85, respectively. Use the following formula for linear interpolation calculation:

$$f_{size}=0.90-\frac{19-18}{20-18}\times(0.90-0.85)=0.875$$

Appendix 8 Region of interest (ROI) placement rationale

In this study, a ROI with an area of 20 mm² was selected for the measurement of CT value and SD value according to the following criteria:

Firstly, to mitigate the partial volume effect. The 20 mm² ROI size is appropriate for pediatric chest CT examinations (with a slice thickness of 1.25 mm). It offers an adequate number of pixel units to encompass the target tissues (normal lung parenchyma and multiple alveolar lesions), while circumventing the partial volume effect induced by an overly small ROI, thus ensuring the accuracy of CT value and SD measurements.

Secondly, to ensure the consistency and repeatability of measurement operations. The fixed ROI size eliminates the influence of radiologists' subjective selection of ROI size on the measurement results, guaranteeing both inter-observer and intra-observer consistency in quantitative assessment.

Thirdly, to conform to clinical applicability. This ROI size is in accordance with the Regional Standard for Quantitative Assessment of Chest CT Image Quality recommended by the Radiological Society of North America (RSNA), ensuring the comparability of the study results with other relevant research.

Fourthly, the ROI localization method adheres to a standardized procedure. The CT cross-section containing the MPP lesion is chosen as the standard slice. The ROI is then positioned separately in the normal lung parenchyma region (devoid of lesions, blood vessels, or bronchi) and the typical MPP lesion region (patchy ground-glass opacity [GGO] or mild consolidation) on the same slice. The copy function of the workstation is utilized to localize the ROI at the same size and position in the corresponding regions of three consecutive cross-sections, thereby avoiding manual operational errors.

Appendix 9 Clinical interpretation of negative lung parenchyma SNR value

The pulmonary parenchyma is a low density tissue within the human body. Under the standard calibration of CT values (where water is defined as 0 HU and air as –1,000 HU), its CT value is negative (in this study, ranging from –1,000 to –700 HU). The SD value, which represents noise, is an absolute positive value. The ratio of the negative CT value to the positive SD value leads to a negative SNR value for the pulmonary parenchyma.

The negative SNR value is a normal outcome in the quantitative assessment of the pulmonary parenchyma in chest CT. The magnitude (absolute value) of this negative SNR serves as a crucial index for reflecting the SNR level. Specifically, the larger the absolute value of the negative SNR, the higher the SNR of the pulmonary parenchyma, and the better the image quality of the normal pulmonary parenchyma.

Appendix 10 Two standardized stages of the qualitative evaluation of image quality

Before the formal evaluation, two radiologists conducted unified training on the qualitative evaluation criteria of pediatric MPP low-dose chest CT images. They performed visual evaluation of the chest CT images of additional 50 pediatric MPP patients who were not included in this study. Consensus results were reached after discussion or consultation with superior doctors when differences arose.

And then, the two independent radiologists assessed the quality of six sets of reconstructed images using a standardized 5-point scoring method for all enrolled patients qualitatively. The radiologists were allowed to scroll and adjust the window level and width (lung window: window width 1500—2000 HU, window level -600—-700 HU; mediastinal window: window width 300—400 HU, window level 30—50 HU) according to clinical diagnostic habits to facilitate the comprehensive assessment of image quality.

The criteria for the 5-point scale are as follows: score 1 = non-diagnostic (severe image noise or artifacts, unable to identify normal lung parenchyma and MPP lesions), score 2 = sub-diagnostic (obvious image noise or artifacts, difficult to identify subtle MPP lesions [e.g., mild GGO]), score 3 = diagnostic (moderate image noise or mild artifacts, normal lung parenchyma and typical MPP lesions can be identified,

https://dx.doi.org/10.21037/tp-2025-1-923

but subtle lesions are not clear), score 4 = good (mild image noise, no obvious artifacts, normal lung parenchyma and all MPP lesions [including subtle lesions] can be clearly identified, and the lesion details are relatively clear), score 5 = excellent (minimal image noise, no artifacts, normal lung parenchyma and MPP lesions can be clearly identified with clear lesion details and good tissue contrast).

Appendix 11 The specific reasons for the exclusion of 93 patients

A total of 93 patients were excluded for the following reasons: 11 for refusing the serum MP-IgM assay or negative MP-IgM results, 7 for incomplete clinical information, 16 for declined or incomplete chest CT examination, 52 for reexamination or non-first admission, 6 for BMI ≥25 kg/m^2, and 1 for failed CT image reconstruction.

Appendix 12 Specific interpretation of observer consistency results

In ASIR-0%, ASIR-50%, ASIR-80%, DLIR-L, DLIR-M, and DLIR-H groups, there were 10, 8, 8, 13, 13, and 7 cases requiring consensus, respectively, of a total of 142 patients included. All these disputes focused on adjacent scores, that is, reviewer 1 has given score-5 while reviewer 2 has given score-4. So far, no score with opposite conclusion has been given. In other words, different reconstruction algorithms were expected to improve the image quality and enhance the diagnostic confidence of radiologists to a certain extent, but we do not think that they have the chance to change the final image diagnosis results. On the other hand, for the six different reconstruction algorithms, the inter-observer consistency was good, and the ICC range is between 0.861 and 0.917 (*Table S4*).

Table S1 Normal distribution test of core indicators

Parameters	D value	P value
Age	0.146	0.002
BMI	0.089	0.087*
WBC	0.141	0.004
CRP	0.189	< 0.001
PCT	0.215	< 0.001
LDH	0.163	< 0.001
$CTDI_{vol}$	0.127	0.007
DLP	0.131	0.005
ED	0.131	0.005
SSDE	0.122	0.010
$SNR_{lung\ parenchyma}$	0.135	0.003
CNR_{MPP}	0.118	0.012
Background noise	0.152	0.001
Subjective score	0.078	0.126*

*, The D value of BMI and subjective scores was < 0.1, with a P value > 0.05, indicating normal distribution. All other parameters did not conform to normal distribution. BMI, body mass index; CNR, contrast-to-noise ratio; CRP, C-reactive protein; $CTDI_{vol}$, the volume CT dose index; DLP, dose-length product; ED, effective dose; LDH, lactate dehydrogenase; MPP, Mycoplasma pneumoniae pneumonia; PCT, procalcitonin; SNR, signal-to-noise ratio; SSDE, size specific dose estimate; WBC, white blood cell.

https://dx.doi.org/10.21037/tp-2025-1-923

Table S2 Correlation between radiation dose parameters and patient body weight

Radiation dose parameter	Correlation coefficient (r)	P value	Correlation strength
$CTDI_{vol}$	0.326	< 0.001	mild positive correlation
DLP	0.358	< 0.001	mild positive correlation
ED	0.358	< 0.001	mild positive correlation
SSDE	0.312	< 0.001	mild positive correlation

$CTDI_{vol}$, the volume CT dose index; DLP, dose-length product; ED, effective dose; SSDE, size specific dose estimate.

Table S3 Pairwise comparisons of subjective scores of both algorithm groups (Bonferroni correction)

Combination of groups	P value	Results
DLIR-H *vs.* ASIR-0%	< 0.001	DLIR-H score was significantly higher
DLIR-H *vs.* ASIR-50%	< 0.001	DLIR-H score was significantly higher
DLIR-H *vs.* ASIR-80%	< 0.001	DLIR-H score was significantly higher
DLIR-H *vs.* DLIR-L	< 0.001	DLIR-H score was significantly higher
DLIR-H *vs.* DLIR-M	< 0.001	DLIR-H score was significantly higher
ASIR-80% *vs.* DLIR-L	0.032	ASIR-80% score was significantly higher
ASIR-80% *vs.* DLIR-M	0.286	no significant differences
Other combinations (e.g., ASIR-50% *vs.* DLIR-L, etc.)	> 0.05	no significant differences

ASIR, Adaptive statistical iterative reconstruction; DLIR, deep learning image reconstruction; DLIR-H, DLIR at high-strength level; DLIR-L, DLIR at low-strength level; DLIR-M, DLIR at medium-strength level.

Table S4 Inter-observer consistency analyses of subjective scores in six different reconstruction algorithms

Reconstruction algorithm	ICC (95% CI)	P value	Consistency degree
ASIR-0%	0.906 (0.871, 0.931)	< 0.001	excellent
ASIR-50%	0.914 (0.883, 0.938)	< 0.001	excellent
ASIR-80%	0.897 (0.858, 0.925)	< 0.001	excellent
DLIR-L	0.868 (0.820, 0.903)	< 0.001	good
DLIR-M	0.861 (0.812, 0.898)	< 0.001	good
DLIR-H	0.917 (0.892, 0.937)	< 0.001	excellent
overall consistency	0.892 (0.865, 0.914)	< 0.001	good

ASIR, Adaptive statistical iterative reconstruction; CI, Confidence interval; DLIR, deep learning image reconstruction; DLIR-H, DLIR at high-strength level; DLIR-L, DLIR at low-strength level; DLIR-M, DLIR at medium-strength level; ICC, intraclass correlation coefficient.

https://dx.doi.org/10.21037/tp-2025-1-923

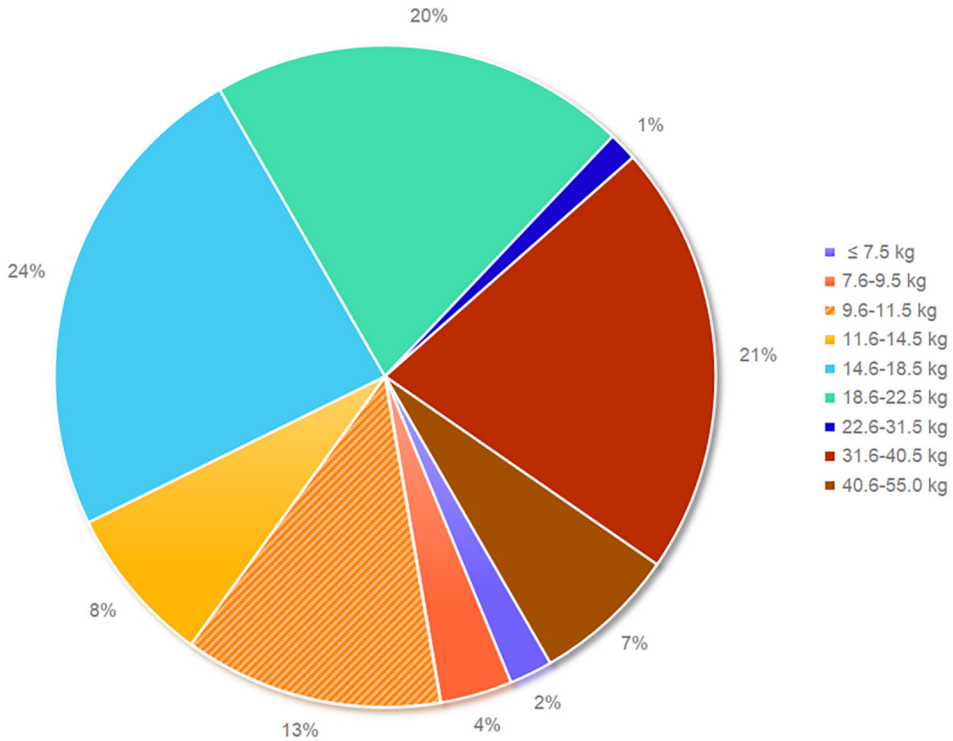

Figure S1 Distribution of enrolled patients by weight range. A pie chart showing the weight stratification of the 142 enrolled pediatric patients: ≤ 7.5 kg (1%), 7.6—9.5 kg (24%), 9.6—11.5 kg (13%), 11.6—14.5 kg (21%), 14.6—18.5 kg (13%), 18.6—22.5 kg (8%), 22.6—31.5 kg (7%), 31.6—40.5 kg (4%), 40.6—55.0 kg (2%). The majority of patients fall within the 7.6—14.5 kg range, reflecting the clinical prevalence of MPP in school-age and preschool children. MPP, *Mycoplasma pneumoniae* pneumonia.

https://dx.doi.org/10.21037/tp-2025-1-923

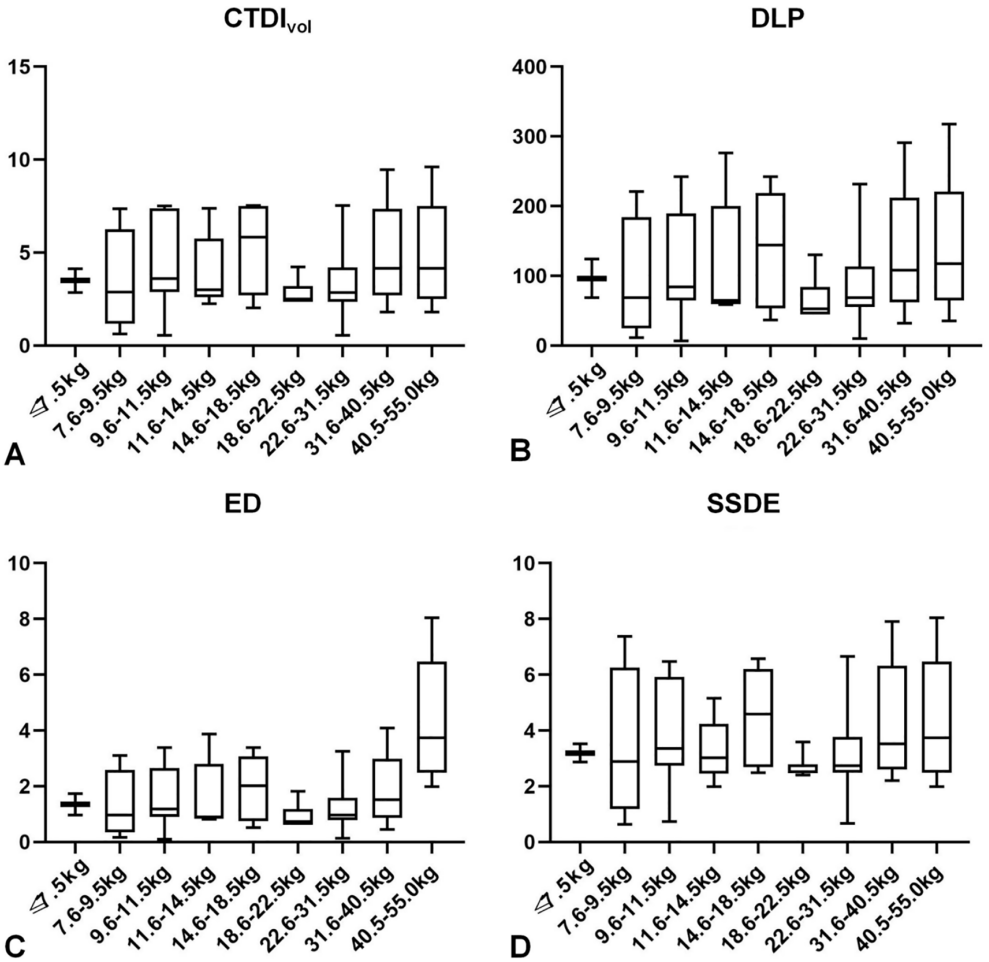

Figure S2 Correlation between radiation dose parameters and patient weight. A scatter plot with linear regression lines showing the mild positive correlation between patient weight and radiation dose parameters: (A) $CTDI_{vol}$ (r = 0.326, P<0.001), (B) DLP (r = 0.358, P<0.001), (C) ED (r = 0.358, P<0.001), (D) SSDE (r = 0.312, P<0.001). Despite the correlation, all dose indices remain below the reference levels recommended in Chinese pediatric CT guidelines, confirming compliance with low-dose requirements even in higher-weight patients. $CTDI_{vol}$, the volume CT dose index; DLP, dose-length product; ED, effective dose; SSDE, size specific dose estimate.

https://dx.doi.org/10.21037/tp-2025-1-923